

August 21, 2002

# RELATIVISTIC SINGULAR ISOTHERMAL TOROIDS

Mike J. Cai

*Department of Physics, University of California  
Berkeley, CA 94720-3411, USA*

mcai@astron.berkeley.edu

Frank H. Shu

*Physics Department, National Tsing Hua University  
Hsinchu 30013, Taiwan, ROC*

fshu@astron.berkeley.edu

## ABSTRACT

We construct self-similar, axisymmetric, time-independent solutions to Einstein's field equations for an isothermal gas with a flat rotation curve in the equatorial plane. The metric scales as  $ds^2 \rightarrow \alpha^2 ds^2$  under the transformation  $r \rightarrow \alpha r$  and  $t \rightarrow \alpha^{1-n} t$ , where  $n$  is a dimensionless measure of the strength of the gravitational field. The solution space forms a two-parameter family characterized by the ratios of the isothermal sound speed and the equatorial rotation speed to the speed of light. The isodensity surfaces are toroids, empty of matter along the rotation axis. Unlike the Newtonian case, the velocity field is not constant on a cylindrical radius because of frame dragging. As the configuration rotates faster, an ergoregion develops in the form of the exterior of a cone centered about the rotation axis. The sequence of solutions terminates when frame dragging becomes infinite and the ergocone closes onto the axis. The fluid velocity of the last solution has a modest value in the midplane but reaches the speed of light on the axis.

## 1. Introduction

In remarkable treatments of the axisymmetric equilibria of self-gravitating, isothermal, unbounded, stellar and gaseous systems with flat rotation curves, Toomre (1982) and Hayashi

et al. (1982) found completely analytical solutions for these self-similar configurations. The theory applies in the non-relativistic limit when mechanics and gravitation can be approached by Newtonian concepts. Written in spherical polar coordinates  $(r, \theta, \phi)$ , the density profile of a Hayashi-Toomre model has the form:

$$\rho(r, \theta) = \left(1 + \frac{V^2}{2a^2}\right)^2 \left(\frac{a^2}{2\pi Gr^2}\right) \csc^2 \theta \operatorname{sech}^2 \left[ \left(1 + \frac{V^2}{2a^2}\right) \ln \cot \frac{\theta}{2} \right], \quad (1-1)$$

where  $V$  is the rotation velocity and  $a$  is the isothermal acoustic (or stellar dispersive) speed. Notice that, apart from a trivial scaling relative to  $a^2$ , the Hayashi-Toomre models form a *linear sequence* characterized by the single value  $V^2/a^2$ . Notice also that  $\rho = 0$  for  $\theta = 0$  or  $\pi$ , whereas  $\rho \rightarrow \infty$  as  $r \rightarrow 0$  and the enclosed mass within a sphere of radius  $r$  goes to infinity as  $r \rightarrow \infty$ . These properties account for our assignment of the name “singular isothermal toroid” (SIT) for this generic class of models (see also Li & Shu 1996).

What is the relativistic generalization of the Hayashi-Toomre sequence when  $a$  and  $V$  are not small compared to the speed of light  $c$ ? In this paper we confirm the intuitive expectation that the linear sequence will broaden into a two-dimensional surface characterized by the pair of dimensionless parameters  $v \equiv V/c$  and  $\gamma \equiv a^2/c^2$ . In the limit  $v^2/\gamma \equiv V^2/a^2 \gg 1$ , we further anticipate that relativistic SITs will become highly flattened, like their non-relativistic analogs in the same limit; i.e., SITs will become SIDs (singular isothermal disks).<sup>1</sup>

Relativistic SIDs have been studied by Cai & Shu (2002, hereafter CS), who took their inspiration from the cold-disk work of Lynden-Bell & Pineault (1978a,b). CS adopted the simplification of negligible disk thickness by assuming an anisotropic pressure tensor, with zero and nonzero effective sound speeds in the vertical and horizontal directions respectively. Part of the rationale for the present investigation is to ascertain the range of validity of the disk approximation when the same effective sound speed  $a$  applies in all three principal-axis directions, and when the combination  $v^2/\gamma$  is not necessarily large compared to unity. In particular, we wish to examine how frame-dragging may distort expectations of toroid flatness formed by naive extrapolations from the Newtonian experience.

The astronomical motivation for the work of Hayashi et al. (1982) and Toomre (1982) comes from interstellar gas clouds and disk galaxies. It is unknown whether such objects have their relativistic counterparts in astrophysics. For example, active galactic nuclei and quasi-stellar objects are increasingly believed to be powered by supermassive blackholes

---

<sup>1</sup>In this paper, we use the terminology “isothermal” somewhat loosely to mean that the pressure is directly proportional to mass density  $\rho$ , with a constant of proportionality that we call  $a^2 \equiv \gamma c^2$ . Such a proportionality can arise, of course, in physical systems in a wider context than when the thermodynamic temperature is a strict constant.

(SMBHs). Are such SMBHs the central products of slow growth through an accretion disk? Or do they result from successive mergers of smaller units (stars or smaller BHs) in the nuclei of galaxies? Or could SMBHs have formed from the monolithic gravitational collapse of relativistically compact gaseous or stellar systems that resemble SITs?

Haehnelt & Kauffmann (2001) discuss the difficulties associated with the first two scenarios. If the last scenario is a viable or even likely possibility, it would be important to develop theoretical predictions and observational tests. Such tests provide another motivation for the present line of research. In particular, it is known that slowly rotating, non-relativistic, gaseous SITs are unstable to inside-out gravitational collapse to form a steadily growing pointlike mass at the center (see, e.g., Shu 1977 for the simplest case of the collapse of a singular isothermal sphere or SIS). The analogous collapse of a suitably flattened, relativistic SIT (during the earliest epochs of galaxy formation) to form a steadily growing SMBH (with a Kerr-like geometry) should be accompanied by the copious generation of gravitational radiation. Such radiation might be detectable by future gravitational-wave observatories.

Differentially rotating objects exemplified by SITs and SIDs have other advantages over the uniformly rotating, relativistic disks investigated in the pioneering work of Bardeen & Wagoner (1971). From numerous studies of self-gravitating systems in the Newtonian regime (see, e.g., Toomre 1977, Binney & Tremaine 1978, Lowe et al. 1994, Bertin et al. 1989ab, Goodman & Evans 1999, Shu et al. 2000), it is known that the transfer of angular momentum from inside to outside through spiral and barlike density waves is a natural phenomenon in configurations that are differentially rather than uniformly rotating. Moreover, for similar distributions of specific angular momentum, differentially rotating systems have lower specific energy, making them more likely states to be encountered in many natural settings (Mestel 1963). These considerations add yet more motivation for the continued theoretical investigation of relativistic SITs and SIDs.

The rest of this paper is organized as follows. In §2, we develop the mathematical equations governing SITs. In §3.1, we solve the Einstein equations in the Newtonian limit and show that the solution thus obtained is identical to those of Toomre (1982) and Hayashi et al. (1982). In §3.2 we derive analytical solutions for relativistic SISs when spherical symmetry holds. §4 describes the numerical strategy we use to solve the fully nonlinear Einstein equations in the presence of finite rotation. §5 summarizes the results of our calculations, including the three dimensional velocity field and the degree of flattening due to rotation. Finally, we offer conclusions and commentary in §6.

## 2. Basic Equations

### 2.1. Metric

Unlike the razor-thin disks studied in CS, we wish to consider pressure tensors in this paper that are isotropic in three dimensions. In spacetime, the stress-energy tensor is then a smooth function of polar angle  $\theta$ , being positive-definite from pole to equator, with reflection symmetry about the latter. Because the sources of gravity are smoother than a delta function, the functions,  $N(\theta)$ ,  $P(\theta)$ ,  $Q(\theta)$ , and  $Z(\theta)$  in the the metric adopted by CS,

$$ds^2 = -r^{2n}e^N dt^2 + r^2e^{2P-N}(d\phi - r^{n-1}e^{N-P}Qdt)^2 + e^{Z-N}(dr^2 + r^2d\theta^2), \quad (2-1)$$

have no kinks as we cross the midplane, unlike the disk case. For clarity, we recapitulate a few important properties of this metric.

In the above equation  $n$  is a number between 0 and 1, which we call the gravitational index. In our choice of coordinates (but not in Lynden-Bell & Pineault 1978a,b), the radial coordinate  $r$  has the usual dimensions of length. The presence of the extra factor  $r^n$  in front of each power of  $dt$  would then seem to indicate that  $t$  does not have the unit of length (in geometric units where  $c = G = 1$ ). This impression is mistaken. As explained in CS, the gravitational potential of self-similar SISs, SIDs, or SITs have logarithmic dependences on the radial coordinate  $r$ . For example, except for slight notational modifications, Toomre (1982) and Hayashi et al. (1982) found that the gravitational potential associated with the density distribution (1-1) is given in conventional units by

$$\Phi = (V^2 + 2a^2) \ln r + \frac{1}{2}c^2 N(\theta),$$

where  $N(\theta)$ , up to an additive constant, has a functional form that can be obtained by integration of the expression for  $N'$  to be given in §3.1. When exponentiated, as in  $g_{tt} = -e^{2\Phi/c^2} = -r^{2n}e^N$  with  $n = v^2 + 2\gamma$ , this logarithmic dependence yields one troublesome factor of  $r^n$  for each index of  $t$  involved in a metric coefficient associated with the differential of time. However, an arbitrary length scale  $L$  introduced to make the argument of the logarithmic term formally dimensionless, i.e., to convert  $\ln r$  to  $\ln(r/L)$  would add an arbitrary constant to the potential  $\Phi$  that would have no physical consequences. The factors of  $r^n$  or  $r^{2n}$  then become the dimensionless combinations  $(r/L)^n$  or  $(r/L)^{2n}$ , which would restore to time  $t$  its usual unit. The arbitrariness of  $L$  then merely reflects the freedom to scale in a problem that is self-similar and lacks intrinsic length scales. For notational compactness, we have adopted the convention of setting  $L$  equal to unity. In any contour-level figure, therefore, the reader can make whatever length assignment she or he might like to any given contour, and scale all other contours accordingly. (Except for size, they all look the same.)

The coordinate  $\theta$  differs from the normal definition of colatitude by a constant factor  $k \geq 1$  (see again the discussion of CS). If  $\theta$  were defined as usual to have a range from 0 to  $\pi$  (as in Lynden-Bell & Pineault 1978a,b),  $k$  would appear elsewhere in the problem as an eigenvalue to be found by satisfying certain boundary conditions. Such eigenvalue searches in nonlinear differential equations are numerically very expensive. By absorbing the factor  $k$  into the definition of  $\theta$ , we change the nature of the eigenvalue search to placing the midplane in a proper location  $\theta_0 \neq \pi/2$ . Determining the value of  $\theta_0$  turns out to be possible via a computationally non-taxing shooting scheme in our formulation of the numerical solution of the Einstein equations.

Physically, the point is as follows. The gravitation of a flattened distribution of matter curves space in such a way as to warp the polar angle  $\theta$  if we choose  $e^{[Z(\theta)-N(\theta)]/2}r$  to be the radial distance from the origin along any path of constant  $t$ ,  $\phi$  and  $\theta$ . (The assumption of axial symmetry allows us to preserve the usual meaning of the azimuthal angle  $\phi$ .) This warping is such as to make the total angle coverage from north rotational pole to south rotational pole greater than  $\pi$  (but always less than  $2\pi$ ).

Apart from the transformations described above, the metric (2-1) has the only form consistent with the requirements of self-similarity, i.e., it satisfies the scaling law  $ds^2 \rightarrow \alpha^2 ds^2$  when  $r \rightarrow \alpha r$ , and  $t \rightarrow \alpha^{1-n}t$  for a constant  $\alpha$ . As explained in CS, the scaling of  $t$  arises from the gravitational redshift associated with climbing out of the potential of this problem. Limiting the effect to redshifts then imposes the allowable range  $0 \leq n \leq 1$ , as we noted earlier and as will be confirmed in detail later.

## 2.2. Einstein's Equations

We denote ordinary differentiation by  $\theta$  with a subscript in this variable, and define  $\mathcal{R}_{(a)(b)} \equiv r^2 e^{Z-N} R_{(a)(b)}$ , where  $R_{(a)(b)}$  is the usual Ricci tensor. We adopt as a convention that numerical indices or indices in parentheses are tetrad indices, which are raised and lowered with the Minkowski metric, while Greek indices are vector indices and are raised and lowered with the metric coefficients of equation (2-1). In this notation, the scaled Ricci

tensor resulting from the metric (2-1) has the nontrivial components:

$$\begin{aligned}
2\mathcal{R}_{(0)(0)} &= N_{\theta,\theta} + N_\theta P_\theta + 2n(1+n) - Q^2\{[(\ln Q)_\theta - P_\theta + N_\theta]^2 + (1-n)^2\}, \\
2\mathcal{R}_{(0)(1)} &= Q_{\theta,\theta} + Q_\theta P_\theta - Q[P_{\theta,\theta} - N_{\theta,\theta} + (P_\theta - N_\theta)^2 + P_\theta(P_\theta - N_\theta) + 2(1-n)], \\
\mathcal{R}_{(0)(0)} - \mathcal{R}_{(1)(1)} &= P_{\theta,\theta} + P_\theta^2 + (n+1)^2, \\
2\mathcal{R}_{(2)(2)} &= N_{\theta,\theta} - Z_{\theta,\theta} + P_\theta(N_\theta - Z_\theta) + 2n(1-n) + Q^2(1-n)^2, \\
2\mathcal{R}_{(2)(3)} &= (n+1)Z_\theta - 2nN_\theta + Q^2(1-n)[P_\theta - (\ln Q)_\theta - N_\theta], \\
2[\mathcal{R}_{(3)(3)} + \mathcal{R}_{(0)(0)} - \mathcal{R}_{(1)(1)} - \mathcal{R}_{(2)(2)}] &= 2P_\theta Z_\theta - N_\theta^2 + 4n^2 + Q^2\{[N_\theta + (\ln Q)_\theta - P_\theta]^2 - (n-1)^2\},
\end{aligned} \tag{2-2}$$

in the locally nonrotating observer (LNRO) frame defined as usual by

$$\begin{aligned}
e_{(0)}^\mu &= (r^{-n}e^{-\frac{1}{2}N}, r^{-1}Qe^{\frac{1}{2}N-P}, 0, 0), \\
e_{(1)}^\mu &= (0, r^{-1}e^{\frac{1}{2}N-P}, 0, 0), \\
e_{(2)}^\mu &= (0, 0, e^{\frac{1}{2}(N-Z)}, 0), \\
e_{(3)}^\mu &= (0, 0, 0, r^{-1}e^{\frac{1}{2}(N-Z)}).
\end{aligned} \tag{2-3}$$

For the matter part, we adopt an isotropic pressure. The pressure  $p$  and energy density  $\varepsilon$  are related by

$$p = \gamma\varepsilon, \tag{2-4}$$

where  $\sqrt{\gamma}$  is the sound speed. (In conventional units,  $\varepsilon = \rho c^2$ , and  $a^2 = \gamma c^2$ .) In an equilibrium solution, there is no vertical or radial velocity, and we may write in the LNRO frame

$$u^{(a)} = \left( \frac{1}{\sqrt{1-v^2}}, \frac{v}{\sqrt{1-v^2}}, 0, 0 \right). \tag{2-5}$$

Unlike the Newtonian case, where the Poincaré-Wavré theorem ensures that the velocity field is independent of  $z$  in cylindrical coordinates (e.g., Tassoul 1978), we will have to assume here the velocity  $v$  is a function of the polar angle  $\theta$ . For a perfect fluid, the stress energy tensor is given by

$$T_{(a)(b)} = (\varepsilon + p)u_{(a)}u_{(b)} + p\eta_{(a)(b)} \tag{2-6}$$

Explicitly, the non-zero components are

$$\begin{aligned}
T_{(0)(0)} &= \varepsilon \frac{1+\gamma v^2}{1-v^2}, & T_{(0)(1)} &= -\varepsilon \frac{(1+\gamma)v}{1-v^2}, \\
T_{(1)(1)} &= \varepsilon \frac{\gamma+v^2}{1-v^2}, & T_{(2)(2)} &= \gamma\varepsilon = T_{(3)(3)}.
\end{aligned} \tag{2-7}$$

The equation of motion  $T^{(a)(b)}_{|(b)} = 0$  has two nontrivial components:

$$\begin{aligned} (\hat{r}) : \quad & -n + v^2 + 2\gamma \frac{1-v^2}{1+\gamma} + Qv(1-n) = 0, \\ (\hat{\theta}) : \quad & v(Q+v)P_\theta - vQ_\theta - (\ln \varepsilon)_\theta \gamma \frac{1-v^2}{1+\gamma} - \frac{1}{2}N_\theta(1+v^2+2Qv) = 0. \end{aligned} \quad (2-8)$$

The first equation yields radial force balance: with  $-n$  representing gravity;  $v^2$  representing centripetal acceleration (a factor  $1/r$  has been cancelled from all terms);  $2\gamma(1-v^2)/(1+\gamma)$  representing the pressure gradient (the factor 2 comes from differentiating a pressure that is proportional to  $r^{-2}$  while the factor  $(1-v^2)/(1+\gamma)$  comes from making various inertial corrections); and  $Qv(1-n)$  representing the effect of the dragging of inertial frames. The second equation describes a similar balance in the  $\theta$  direction. In the problem of an infinitesimally thin disk, both equations are evaluated on the equatorial plane only. If we then impose symmetry about the equator, the second equation is identically satisfied upon integrating across the mid-plane. For the 3-D configuration we are considering here, the second equation provides a non-trivial consistency relationship for the energy density.

To proceed further, let us define

$$\hat{\varepsilon} = 8\pi r^2 \frac{\varepsilon}{(1+n)^2} e^{Z-N}, \quad \Theta = (1+n)\theta, \quad (2-9)$$

and denote differentiation with respect to  $\Theta$  by primes. The Einstein equations may now be written as

$$R_{(a)(b)} = 8\pi \left[ T_{(a)(b)} - \frac{1}{2}\eta_{(a)(b)}T \right]. \quad (2-10)$$

Written out in full, the components are

$$\begin{aligned} \hat{\varepsilon} \frac{1-\gamma v^2+3\gamma+v^2}{1-v^2} &= N'' + N'P' + \frac{2n}{1+n} - Q^2 \left\{ [(\ln Q)' - P' + N']^2 + \left( \frac{1-n}{1+n} \right)^2 \right\}, \\ -2\hat{\varepsilon}v \frac{1+\gamma}{1-v^2} &= Q'' + Q'P' - Q \left[ P'' - N'' + (P' - N')^2 + P'(P' - N') + \frac{2(1-n)}{(1+n)^2} \right], \\ 2\gamma\hat{\varepsilon} &= P'' + P'^2 + 1, \\ (1-\gamma)\hat{\varepsilon} &= N'' - Z'' + P'(N' - Z') + \frac{2n(1-n)}{(1+n)^2} + Q^2 \left( \frac{1-n}{1+n} \right)^2, \\ 0 &= Z' - \frac{2n}{1+n}N' + Q^2 \frac{1-n}{1+n} [P' - (\ln Q)' - N'], \\ 4\gamma\hat{\varepsilon} &= 2P'Z' - N'^2 + \left( \frac{2n}{1+n} \right)^2 + Q^2 \left\{ [N' + (\ln Q)' - P']^2 - \left( \frac{1-n}{1+n} \right)^2 \right\}. \end{aligned}$$

With some algebra, we may separate out a part of Einstein's equations and the equation of motion (2-8) to put them into a set of “dynamical” equations involving second- and first-order derivatives, respectively, of metric and matter variables:

$$N'' = \hat{\varepsilon} \frac{1 - \gamma v^2 + 3\gamma + v^2}{1 - v^2} - N'P' - \frac{2n}{1 + n} + F^2 + Q^2 \left( \frac{1 - n}{1 + n} \right)^2, \quad (2-11a)$$

$$Q'' = -\hat{\varepsilon}(2v + Q + Qv^2) \frac{1 + \gamma}{1 - v^2} - Q'P' + Q \left[ (1 - Q^2) \left( \frac{1 - n}{1 + n} \right)^2 + (P' - N')^2 - F^2 \right], \quad (2-11b)$$

$$P'' = 2\gamma\hat{\varepsilon} - 1 - P'^2, \quad (2-11c)$$

$$(\ln \hat{\varepsilon})' = \left\{ v^2 P' - vF - \frac{1}{2} N'(1 + v^2) \right\} \frac{1 + \gamma}{\gamma(1 - v^2)} - \frac{1 - n}{1 + n} \{N' - QF\}, \quad (2-11d)$$

where  $F = QN' + Q' - QP'$ . This set of ordinary differential equations (ODEs) is supplemented by a set of constraint equations from the rest of Einstein equations and equations of motion involving only first- and zeroth-order derivatives, respectively, of metric and matter variables:

$$0 = -n + v^2 + 2\gamma \frac{1 - v^2}{1 + \gamma} + Qv(1 - n), \quad (2-12a)$$

$$4\gamma\hat{\varepsilon} = \left( \frac{2n}{1 + n} \right)^2 + P'N' \frac{4n}{1 + n} + F^2 + 2FP'Q \frac{1 - n}{1 + n} - N'^2 - Q^2 \left( \frac{1 - n}{1 + n} \right)^2. \quad (2-12b)$$

Notice that  $Z$  decouples from the other three metric coefficients. Its dynamical ODE can be replaced by one of the equations of motion associated with the contracted Bianchi identity. The function  $Z$  can be easily obtained through integration once the other three metric coefficients  $N$ ,  $P$ , and  $Q$  are found.

Equation (2-12a) for radial force balance has the following important implication:  $v$  cannot be a constant, as in the nonrelativistic case, but must vary with  $\Theta$  if the coefficient governing frame dragging  $Q$  does. Moreover, because  $Q(\Theta)$  must vanish on the rotational poles,  $\Theta = 0$  and  $2\Theta_0$ ,  $v$  will generally *not* be zero at the rotation axis for general  $n$  and  $\gamma$  (e.g.,  $V \neq 0$  for general Hayashi-Toomre SITs). Indeed, because  $(1 - n)$  and  $Q$  are both positive,  $v$  will achieve its greatest value on the rotational pole, where frame dragging cannot help centrifugal forces and pressure gradients to balance self-similar gravity.

As a final comment, notice that although equation (2-12b) can be used to compute energy density  $\hat{\varepsilon}$  on computational grid points, it does not manifestly require a positive definite value for  $\hat{\varepsilon}$ . Fortunately, we know that the other non-trivial contracted Bianchi



identity guarantees that equation (2-12b) is a redundant relationship, given the remaining independent equations of the governing set. Thus, we can use equation (2-11d) to integrate for  $\ln \hat{\varepsilon}$  (always obtaining a positive value  $\hat{\varepsilon}$  no matter what the sign of  $\ln \hat{\varepsilon}$ ), and then check numerically that equation (2-12b) yields a consistent result (which it always does). Thus, the remaining equations (2-11) and (2-12a) form a complete set to determine the spacetime geometry.

### 2.3. Boundary Conditions

The equations (2-11) form a set of first-order non-linear ODEs in the five variables  $\{N', Q, Q', P', \ln \hat{\varepsilon}\}$ . Thus, five boundary conditions will specify a solution. As explained below, we have three boundary conditions each that we desire to impose at the pole and the equator, and therefore we seemingly have an overdetermined situation. In fact, because the location of the equator is not given a priori, we have a well-posed problem.

Let us start with the rotation axis. As usual, one wants a circle in the  $\phi$  direction specified by constant  $\Theta$  to have vanishingly small circumference if  $\Theta \rightarrow 0$ . Thus, we need  $e^P \rightarrow 0$ , which requires  $P$  to go to  $-\infty$  at the pole  $\Theta = 0$ . In order to have a non-singular geometry on the axis, the Ricci tensor must remain finite as  $\Theta \rightarrow 0$ . The boundary conditions on the axis that are compatible with the Newtonian limit are therefore

$$\begin{aligned} N' = 0 : & \quad \text{The gravitational field is smooth across the axis.} \\ Q = 0 : & \quad \text{There is no frame dragging on the axis.} \\ P' = +\infty : & \quad \text{Coordinate singularity.} \end{aligned} \tag{2-13}$$

We noted earlier that the fluid velocity  $v$  is generally non-vanishing on the rotation axis (as is true, e.g., in the Hayashi-Toomre models). We anticipate therefore that the infinite “centrifugal” effect at the pole will drive away all matter from it and create a cavity there (explaining, e.g., why the Hayashi-Toomre configurations are “toroids”). If we suppose that a near-vacuum situation applies also to relativistic SITs and approximate  $\hat{\varepsilon}$  to be vanishingly small near the rotation axis, we can show that equation (2-11d) has the general solution,

$$P = \ln[K \sin(\Theta - \Theta_1)], \tag{2-14}$$

in a small neighborhood of  $\Theta = \Theta_1$  where  $\hat{\varepsilon}$  vanishes, with  $K$  and  $\Theta_1$  being integration constants. The coordinate singularity imposed by  $P'$  being infinite on the north pole then identifies that  $\Theta_1 = 0$ ; i.e.,  $P' \approx 1/\Theta$  for small  $\Theta$ . Notice finally that the divergence of  $P'$  at the north pole is consistent with the vanishing there of the energy density  $\hat{\varepsilon}$  on the

left-hand side of equation (2-11d). Thus, from a physical point of view, we can now see that the boundary conditions  $Q = 0$  and  $P' = +\infty$  at the axis are not two distinct requirements, but only one (once we fix the north pole to be at  $\Theta = 0$ ).

We recapitulate. The condition  $Q = 0$  at the pole makes  $v$  generally nonzero on the axis. A non-vanishing  $v$  on the rotation axis centrifugally expels matter from the region  $\Theta = 0$ . This makes  $\hat{\varepsilon}$  zero, leading to a logarithmic divergence of  $P(\Theta)$  at  $\Theta = 0$  that allows the automatic satisfaction of  $P' = +\infty$  at the north pole, once we have located it properly relative to the equator. The latter can be assured by a proper technique to determine  $\Theta_0$  (see below).

Next, we demand the solution to be symmetric about the midplane. This implies that the first derivatives of metric coefficients have to vanish there. Thus, at the midplane,

$$N' = P' = Q' = 0. \quad (2-15)$$

Notice from equation (2-11d) that  $\varepsilon'$  vanishes automatically once the other three conditions are met. Equations (2-13) and (2-15) are the six boundary conditions referred to at the beginning of this subsection.

### 3. Special Solutions

#### 3.1. Newtonian Limit

Before we describe the numerical procedure and general solution, let us pause to discuss the Newtonian limit, where  $v$  and  $\gamma$  are small compared to unity. This limit should yield Toomre and Hayashi's result. In the Newtonian limit,  $g_{ij}$  approaches the metric of Euclidean space in spherical coordinates;  $g_{0i}$  vanishes; and  $g_{00} \rightarrow -\exp(2\Phi) \sim -1 + O(v^2)$ . In our metric, this procedure translates to

$$\gamma, v^2, \hat{\varepsilon}, N = O(n) \ll 1, \quad \Theta = \theta, \quad \Theta_0 = \frac{\pi}{2}, \quad P = \ln \sin \theta, \quad Q = Z = 0.$$

With these simplifications, Einstein's field equations reduce to the usual Poisson's relation, and the equations of motion recover those of Newtonian fluid dynamics. Instead of (2-11d), we will revert to using (2-12b) to determine the energy density. Equations (2-12a), (2-12b), and (2-11a) now have the approximate forms:

$$\begin{aligned} 0 &= -n + v^2 + 2\gamma \\ \gamma \hat{\varepsilon} &= n^2 + n \cot \theta N' - \frac{1}{4} N'^2, \\ N'' &= \hat{\varepsilon} - N' \cot \theta - 2n. \end{aligned} \quad (3-1)$$

These equations may be combined to give a single nonlinear first-order ODE for  $N'$ :

$$N'' = \left(\frac{n}{\gamma} - 1\right) N' \cot \theta - \frac{1}{4\gamma} N'^2 + \frac{n^2}{\gamma} - 2n, \quad (3-2)$$

to be solved subject to the boundary condition  $N' = 0$  for  $\theta = 0$ . The appropriate solution is then

$$\begin{aligned} n &= v^2 + 2\gamma, \\ \hat{\varepsilon} &= \frac{n^2}{\gamma} \csc^2 \theta \operatorname{sech}^2 \left[ \frac{n}{2\gamma} \ln \cot \frac{\theta}{2} \right], \\ N' &= 2n \left\{ \cot \theta - \csc \theta \tanh \left[ \frac{n}{2\gamma} \ln \cot \frac{\theta}{2} \right] \right\}. \end{aligned} \quad (3-3)$$

The first equation recovers the usual Newtonian simplification for mechanical equilibrium: gravity  $n$  is balanced by centripetal acceleration  $v^2$  and the specific pressure gradient  $2\gamma$ , with no relativistic corrections for inertia or frame dragging. The second and third equations give, respectively, the density distribution (proportional to  $\hat{\varepsilon}$ ) and the self-consistent gravitational field (proportional to  $N'$ ) required to achieve mechanical equilibrium in the  $\theta$  direction. Apart from notational differences, these results are indeed what Toomre and Hayashi found.

For the nonrotating configuration, we expect a spherically symmetric solution. In this limit,  $n = 2\gamma$ , and

$$\hat{\varepsilon} = 4\gamma, \quad N' = 0.$$

Expressed in dimensional variables, this is the familiar result,  $\rho = \varepsilon/c^2 = a^2/2\pi Gr^2$ , appropriate for a SIS.

When there is even a slight amount of rotation,  $n > 2\gamma$ , and  $\hat{\varepsilon} \rightarrow 0$  on the axis. In fact, for  $\theta \ll 1$ ,

$$\hat{\varepsilon} \propto \theta^{n/\gamma-2} \propto \theta^{v^2/\gamma},$$

and curves of constant density  $\rho \propto \hat{\varepsilon}(\theta)/r^2$  follow

$$r \propto \theta^{v^2/2\gamma}. \quad (3-4)$$

Thus, except for a very narrow range of angles in the meridional plane near the pole, where isodensity contours plunge toward the origin, isodensity contours otherwise look nearly circular,  $r \approx \text{constant}$ , when  $v^2/2\gamma \ll 1$ . As  $v^2/2\gamma$  increases because of a greater importance of rotational compared to pressure support, isodensity contours become more flattened toward the equatorial plane. Indeed, the figures in Toomre (1982) and Hayashi et al. (1982) show that the solutions rapidly approach a disk-like solution as one increases the level of rotation to  $v^2/2\gamma \gg 1$ . We expect the same qualitative behavior to extend into the fully relativistic regime.

### 3.2. Relativistic SISs

In the absence of rotation, the general relativistic solution is a spherically symmetric one with  $Q = 0$  and  $v = 0$ . Equations (2-12a) and (2-12b) then yield

$$n = \frac{2\gamma}{1 + \gamma}, \quad \hat{\varepsilon} = \frac{4\gamma}{(1 + 3\gamma)^2}. \quad (3-5)$$

Equation (2-11d) is now trivially satisfied, whereas the right-hand side of equation (2-11a) is identically zero, implying that  $N'$  is a constant. In fact,  $N'$  has to be 0 if we are to satisfy the boundary conditions (2-13) and (2-15). With  $N'$ ,  $Q$ , and  $v$  all zero, the equation for  $Z'$  shows that it is also 0. Without loss of generality, we may then choose the constants  $N$  and  $Z$  themselves to be 0, so that the metric (2-1) involves no extra scale factors in an interpretation of  $r$  as the radial distance from the origin along any path of constant  $(t, \theta, \phi)$ . Thus, the only nontrivial metric coefficient is  $P$ , which satisfies the ODE (2-11c):

$$P'' + P'^2 = -\alpha^2, \quad (3-6)$$

where the positive constant  $\alpha \leq 1$  is defined as

$$\alpha \equiv \sqrt{1 - 2\hat{\varepsilon}\gamma} = \frac{\sqrt{1 + 6\gamma + \gamma^2}}{1 + 3\gamma}. \quad (3-7)$$

Equation (3-6) may be put into the form

$$(e^P)'' = -\alpha^2 e^P, \quad (3-8)$$

and may be integrated, subject to the pole boundary condition  $e^P = 0$  at  $\Theta = 0$ , to yield

$$e^P = A \sin(\alpha\Theta), \quad (3-9)$$

with  $A$  a nonzero constant.

When we apply the equatorial boundary condition,  $P' = 0$  at  $\Theta = \Theta_0$ , we obtain the identification  $\cos \alpha\Theta_0 = 0$ , or

$$\Theta_0 = \frac{\pi}{2\alpha}. \quad (3-10)$$

The only remaining task is to determine the value of the constant  $A$ . We accomplish this task by requiring that, in the presence of spherical symmetry, half the circumference of a great circle in the meridional plane,  $2r\theta_0 = 2r\Theta_0/(1+n)$  according to the metric (2-1), must be equal to half the circumference of a great circle in the equatorial plane,  $\pi r e^{P(\Theta_0)} = A\pi r$ . This equality generates the identification,

$$A = \frac{1}{\alpha(1+n)} = \frac{1+\gamma}{\sqrt{1+6\gamma+\gamma^2}} \leq 1. \quad (3-11)$$

Thus, the ratio of the circumference of a great circle  $2A\pi r$  to its radius  $r$  from the origin is less than  $2\pi$  for a relativistic SIS with  $\gamma > 0$ . This is a familiar result known for relativistic, self-gravitating, pressure-supported (and therefore spherically symmetric) equilibria, but it is usually derived for Schwarzschild (or Oppenheimer-Volkoff) coordinates, where  $2\pi r_S$  is *defined* as the circumference of a great circle, and  $r_S$  is *not* the true radial distance from the origin. What appears as distortions of angles in our metric (e.g.,  $\theta_0 \geq \pi/2$  is the “angle” between pole and equator) transforms as distortions of the radial dimension in the Schwarzschild metric. If we were to adopt the Schwarzschild description for angles, the radial distance  $r$  to the origin would turn out to be a power law of  $r_S$ , with an exponent different from unity.

As a check that our definitions of  $\theta$  and  $\phi$  lead to no true distortions of angular relationships in the spherically symmetric case, we note that the surface area of a sphere can be calculated from the metric (2-1) as

$$2r^2 \int_0^{2\pi} d\phi \int_0^{\theta_0} e^P d\theta = \frac{4\pi r^2}{1+n} \int_0^{\Theta_0} A \sin(\alpha\Theta) d\Theta = \frac{4\pi r^2}{\alpha^2(1+n)^2}. \quad (3-12)$$

If we compare this formula to the circumference of a great circle  $2\pi r/\alpha(1+n)$ , we note that the ratio of the surface area of a sphere to the square of the circumference of a great circle on the surface of that sphere equals  $1/\pi$ , the same relation as for Euclidean geometry (QED). Angles (polar and azimuthal) maintain their usual relations; it is only the radial direction that suffers true distortion in a relativistic SIS. This completes our discussion of SITs with analytically soluble forms.

#### 4. Numerical Solution

From dimensional considerations, the solutions for rotating SITs form a two-parameter family. The equation of state is a result of microscopic physics, which is independent of the macroscopic spacetime geometry. Thus, the square of the isothermal sound speed,  $\gamma$ , is a natural choice for one of the parameters. The other convenient constant of the problem,  $n$ , measures the strength of the gravitational field. Ideally, we might have preferred to specify in advance the amount of rotation. However, this is inconvenient as  $v$  is a function of “polar angle”  $\Theta$ . We therefore fix on  $\gamma$  and  $n$  to parameterize our solutions, and let this combination determine implicitly the amount of rotation on the equator and elsewhere.

To implement a practical numerical scheme, we solve equation (2-12a) as a quadratic relation for  $v$  to obtain

$$v = \frac{-Q(1+\gamma)(1-n) + \sqrt{(1+\gamma)^2(1-n)^2Q^2 + 4(1-\gamma)(n+n\gamma-2\gamma)}}{2(1-\gamma)}. \quad (4-1)$$

Using the above relation, we compute  $v(\Theta)$  from  $Q(\Theta)$  at every step for use in equations (2-11). Causality demands  $v < 1$  and  $\gamma < 1$ , and  $Q$  must have the same sign as  $v$ , which is taken to be positive by convention. Thus, the solution space is constrained to satisfy

$$0 \leq \gamma \leq 1, \quad \frac{2\gamma}{1+\gamma} \leq n \leq 1. \quad (4-2)$$

In fact,  $(1+\gamma)/(1-\gamma)$  times  $n - 2\gamma/(1+\gamma)$  is the value of  $v^2$  at the pole.

For convenience, we start at the midplane. Because the governing ODEs, equations (2-11) and (2-12), contain no coefficients that depend explicitly on  $\Theta$  itself, these equations are formally invariant to an overall translation of the value of  $\Theta$  at the midplane. Thus, a simple transformation of variables from  $\Theta$  to  $\Psi \equiv \Theta - \Theta_0$  means that we do not need to guess a value of  $\Theta_0$  at the equator, but can obtain it afterwards when we reach the pole, as defined by the value of  $-\Psi$  where  $Q = 0$  is reached. Attainment of  $Q = 0$  at the pole leads to the automatic satisfaction there of  $P' = +\infty$  as we discussed earlier.

The boundary conditions (2-15) define the corresponding values of  $N'$ ,  $P'$ , and  $Q'$  at the new midplane label  $\Psi = 0$ . In principle, we need to guess midplane values of  $Q$  and  $\hat{\varepsilon}$  to begin the integration toward the north pole. In practice, we can eliminate the need to guess  $\hat{\varepsilon}$  at the equator, and use equation (2-12b) to obtain this value, given  $\gamma$  and  $n$ . Thus, we are left with a one-dimensional shooting task of adjusting a guessed midplane value of  $Q = q$  to satisfy the boundary condition  $N' = 0$  at the pole  $\Psi = -\Theta_0$ . Since we want the local energy density to be positive in equation (2-12b), a useful value of  $q$  must reside within the interval:

$$0 \leq q \leq \frac{2n}{1-n}. \quad (4-3)$$

A slight difficulty enters to complicate the above program that deserves mention. When regarded as a function of  $q$ , the relevant zero of  $N'(\Theta)$  turns out to be a double root; i.e.,  $\partial N'(\Theta = 0)/\partial q = 0$  at the sought-after value of  $q$ . We therefore numerically compute  $\partial N'(\Theta = 0)/\partial q$  and refine the grid of possible  $q$  values when this quantity becomes small, so as not inadvertently to jump over the root of  $N'(\Theta = 0)$ .

## 5. Results

To make meridional cross-sectional plots of isodensity surfaces, we use “cylindrical” coordinates  $(t, \varpi, \phi, z)$  that are the counterparts of the system used by Lynden-Bell & Pineault (1978a,b):

$$\varpi = r^{1/k} \sin(\theta/k), \quad z = r^{1/k} \cos(\theta/k), \quad (5-1)$$

where

$$k \equiv \frac{2}{\pi} \theta_0 \quad (5-2)$$

is the factor  $\geq 1$  for the models of this paper discussed in §2.

In these coordinates the metric reads

$$ds^2 = -(\varpi^2 + z^2)^{kn} e^N dt^2 + (\varpi^2 + z^2)^k e^{2P-N} [d\phi - (\varpi^2 + z^2)^{k(n-1)/2} e^{N-P} Q dt]^2 + k^2 (\varpi^2 + z^2)^{k-1} e^{Z-N} (d\varpi^2 + dz^2), \quad (5-3)$$

with the  $\theta$  dependences of the metric coefficients  $N(\theta)$ ,  $P(\theta)$ ,  $Q(\theta)$ ,  $Z(\theta)$  now to be interpreted by making the substitution

$$\theta = k \arctan(\varpi/z). \quad (5-4)$$

Because of spatial curvature, *faithful* representations of both lengths and angles (in the meridional plane) would require curved sheets of paper or a 3-D embedding diagram. Conventional publishing limitations restrict our ability to do full justice to such possible graphical representations, and we have compromised by making  $(\varpi, z)$  plots of the isodensity contours using the coordinate definitions (5-1). We emphasize, however, that when  $n$  is not small (i.e., when gravity is not weak), such plots give graphical relationships of isodensity contours for the *coordinate labels only*, and do not accurately represent spatial separations or angles. Figure 1 gives such plots for the case  $\gamma = 1/3$  (e.g., an ultrarelativistic *ideal* gas whether “isothermal” or not) when  $n$  ranges from a minimum value  $n = 1/2$ , corresponding to no rotation (i.e., a SIS), to a value close to the maximum value  $n = 1$ , corresponding to the most rapidly rotating SIT possible.

When we introduce rotation,  $\hat{\varepsilon}$  has to vanish on the axis as a result of the centrifugal emptying process described earlier. Near the pole, we assume  $\hat{\varepsilon} \propto \Theta^\lambda$  for  $\lambda > 0$ , and adopt a series expansion for  $P'$ , using the “dynamical” equations (2-11):

$$P' = \frac{1}{\Theta} + O(\Theta), \quad \lambda = \left( \frac{v^2}{\gamma} \right) \left( \frac{1 + \gamma}{1 - v^2} \right) = \frac{n + n\gamma - 2\gamma}{\gamma(1 - n)} = \frac{1 + \gamma}{\gamma(1 - n)} (n - n_{\min}),$$

where we have used equation (2-12a) on the axis. Notice that in our constrained solution space (4-2),  $\lambda \geq 0$ . For a slight rotation,  $\lambda \ll 1$ , the power-law behavior of the energy density near the axis causes it to change at a normalized radius from 1 to 0 nearly discontinuously as the pole is approached. This behavior is depicted in Figure 2. Expressed differently, the parameter  $\lambda$  controls the slope of isodensity contours near the pole. As  $\lambda \rightarrow 0^+$ , the isodensity curve in the meridional plane switches from being horizontal to being vertical very quickly as the curve approaches the origin (see Fig. 1). Although  $\hat{\varepsilon}$  has to vanish formally on the axis, Figure 1 shows isodensity contours essentially to be spherical when  $\lambda$  is small.

In general, for positive values of  $\gamma < 1$ ,  $\lambda$  ranges from 0 for the minimum allowed gravitational index  $n$  (and no rotation) to  $\infty$  for  $n = 1$ , which is the maximum gravitational field strength allowed by causality. When  $\gamma = 1$ , a limiting process is required. If we take the limit  $\gamma \rightarrow 1$  first, then we are forced to take  $n = 1$ , and we recover the nonrotating solution of a self-similar sphere with  $\lambda = 0$ . However, if we fix  $n = 1$  and let  $\gamma \rightarrow 1$ , then the result is a maximally rotating SIT with  $\lambda = \infty$ . This ambiguity is a manifestation of the sphere-toroid transition at zero rotational velocity discussed earlier.

From a purely mathematical point of view, the double-limit ambiguity arises because of the non-uniform convergence of solutions towards the singular point  $n = \gamma = 1$ . After all, the Einstein equations formally allow solutions with  $n > 1$ . However, these spacetimes are acausal and have divergent energy density on the axis, and thus are irrelevant for physical considerations. We shall not digress further on this issue. In the following analysis, it is understood that we always take  $\gamma \rightarrow 1$  first.

### 5.1. Velocity Field

With the three-dimensional solutions, we have a chance to study the velocity field as a function of polar angle. In a disk of infinitesimal thickness, for each value of  $\gamma$ , the rotation speed in the plane of the disk is limited to a maximum value that arises when the frame dragging becomes infinite:  $Q \rightarrow \infty$  accompanied by  $n \rightarrow 1$ . Empirically, CS (see their Table 1) found the maximum rotational velocity for a disk to be a function of  $\gamma$  given approximately by

$$v_c = \frac{1}{2.294 + 1.091\gamma}. \quad (5-5)$$

The fact that the maximum velocity *any* disk can have is only about 43.8% of the speed of light came as a surprise when Lynden-Bell & Pineault (1978b) first discovered it for a cold disk, and it has remained a mystery until now.

Three-dimensional SITs are more realistic systems than completely flattened SIDs (with their infinitesimal thickness resulting from an artificial imposition of a highly anisotropic pressure tensor). In a SIT, as seen in Fig 3, the velocity field increases towards the axis, reaching a significant fraction of the speed of light in most cases. This qualitative result was anticipated by our previous discussion. The maximum of the velocity field occurs on the axis where  $Q = 0$  and is given by equation (4-1) as

$$v_{\text{axis}}^2 = \frac{n + n\gamma - 2\gamma}{1 - \gamma}.$$

For a fixed value of  $\gamma \in [0, 1)$ ,  $v_{\text{axis}}$  increases from 0 for minimum rotation to 1 (the speed



of light) for the ultrarelativistic limit. The sequence is then terminated while the equatorial velocities are still a minor fraction of the speed of light, comparable, in fact to the subluminal values given by equation (5-5) for the pure-disk solutions. (For more precise comparisons, see below.) The naive expectation that relativity sets limitations on physical systems only because matter acquires velocities approaching the speed of light is indeed met for SITs where models terminate when (vanishingly small amounts of) gas near the pole become ultra-relativistic. It is only SIDs that present an apparent puzzle because the assumption of a vacuum above and below the exact midplane of the disk removed all material tracers of this ultra-relativistic motion a priori!

The restriction of equatorial rotation velocities to modest fractions of the speed of light implies that differentially rotating, gaseous configurations with isotropic pressure contributing a significant fraction of the total support against self-gravity, cannot be too highly flattened. Despite this caveat, however, it is remarkable how useful the approximation of a disk-like geometry can be to predict certain physical characteristics of more realistic systems. In Table 1, we tabulate as a function of  $\gamma$  the maximum equatorial velocity  $v_c$  attainable by a SID or SIT when the gravitational field acquires the maximum index  $n = 1$  (reached by extrapolation from values of  $n$  somewhat smaller than unity). From this tabulation, we see that the two values of  $v_c$  are in very good agreement when  $\gamma \ll 1$ . This is a natural result because the critically rotating SIT is extremely flattened at low levels of pressure support. However, the good agreement persists to relativistic values of  $\gamma \approx 0.5$ , a surprise since  $v_c^2/\gamma$  is far from being large compared to unity, as is required formally for the disk approximation to hold. Indeed, complete breakdown of the disk approximation does not occur in the Table until  $v_c^2/\gamma$  is significantly *smaller* than unity. Recalling that the ratio of pressure to energy density (including rest mass) is given by  $\gamma = 1/3$  for ultrarelativistic ideal gases, we see that Table 1 implies excellent agreement in the gross properties of SITs and SIDs with realistic equations of state which are maximally rotating. (The apparent discrepancy at  $\gamma = 0$  arises from an imperfect extrapolation of SITs to this limit.) This finding relieves some of the worries that one might otherwise have about the applicability of results derived from a flat disk analysis when parameters are used that would give such disks appreciable vertical thickness if the pressure were isotropic rather than anisotropic (see the caveats expressed in CS).

## 6. Conclusion and Commentary

With the aid of self-similarity, we have constructed a two parameter family of semi-analytic solutions to the Einstein field equations, parameterized by the gravitational index and an isotropic pressure. The isodensity surfaces are toroids, qualitatively similar to their

Newtonian counterparts (Toomre 1982, Hayashi et al. 1982).

The main difference between relativistic SITs and their non-relativistic counterparts is that the former do not satisfy, even approximately, the Poincaré-Wavré theorem (see, e.g., Tassoul 1978). In the Newtonian limit, Goldreich & Schubert (1967) have shown that equilibria which violate the constraint of isorotation on cylinders are unstable on timescales that range from dynamical to secular. It is not known whether such instabilities persist into the relativistic regime if the cause of the departures from isorotation on cylinders is the dragging of inertial frames. This issue deserves further investigation.

We have also gained insight into how frame dragging figures prominently into another puzzle. Lynden-Bell & Pineault (1978b) found, and CS confirmed, that the rotational velocities of completely flat, relativistic disks are limited to be less than 0.438 times the speed of light. This limitation appears quite peculiar, but when we examine the behavior of three-dimensional toroids, the velocity field turns out, as summarized above, to be a function of the polar angle. While the equator is still rotating modestly (subluminally), the velocity on the axis can reach the speed of light when an appropriate combination of parameters holds. As a result, matter is pushed away from the axis much more strongly than one might have suspected by examining only the ratio of rotational support  $v^2$  on the midplane to the pressure contribution  $\gamma$ . As a byproduct, a disklike approximation still holds for many SITs to a surprisingly good degree when one might otherwise have expected a complete breakdown of such a simplified description.

The direct applicability of relativistic SITs and SIDs to realistic astrophysical systems is questionable. They have inner and outer singularities (infinite central density, divergent enclosed mass at infinity) that lead to spacetime geometries (quasi-naked singularity at the origin, nonflat spacetime asymptotically) which are conventionally rejected as inapt descriptions of reality. However, we note that the issue of the possibility of naked singularities in the universe has not been settled in any definitive form (Penrose 1998), and non-asymptotically flat spacetimes are a common feature of many standard cosmologies, including the currently favored versions of accelerating universes with positive cosmological constants. Moreover, for a problem to be interesting in general relativity, spacetime has to possess curvature. But self-similar spacetimes that have power law dependences on some radial coordinate are guaranteed to run into trouble at small and large radii, since the interesting curvature in the body of the problem has to be carried into the origin and to infinity (where they become “objectionable”).

Our point here is not to argue for the direct application of the self-similar models of the current line of research to any known astrophysical object, but to point out their possible utility in the study of a restricted but extremely interesting subset of problems

in general relativity: the role of frame dragging, nontrivial equilibria with and without convenient symmetries, gravitational collapse, the formation of singularities, the efficiency of the generation of gravitational radiation, etc. Computational results in this field are hard to obtain as it is; we should not shrink from applying a technique – self-similarity – that has proven itself very fruitful in application to many subjects other than general relativity, simply because its assumption produces a few blemishes in otherwise acceptable physical models.

This work has been supported in the United States by the National Science Foundation by a Graduate Fellowship awarded to MJC and by grant AST-9618491 awarded to FHS. In Taiwan, we are pleased to acknowledge the support of the National Science Council.

## REFERENCES

- Bardeen, J. & Wagoner, R.: 1971, *Astrophys. J.* **167**, 359.
- Bertin, G., Lin, C. C., Lowe, S. A., & Thurstans, R. P.: 1989a, *Astrophys. J.* **338**, 78.
- Bertin, G., Lin, C. C., Lowe, S. A., & Thurstans, R. P.: 1989b, *Astrophys. J.* **338**, 104.
- Binney, J. & Tremaine, S.: 1987, *Galactic Dynamics*, (Princeton: Princeton University Press).
- Cai, M. J. & Shu, F. H.: 2002, *Astrophys. J.* **567**, 477.
- Goldreich, P. & Schubert, G.: 1967, *Astrophys. J.* **150**, 571.
- Goodman, J. & Evans, N. W.: 1999, *Mon. Not. R. Astron. Soc.* **309**, 599.
- Haehnelt, M. & Kauffmann, G.: 2001, *Black Holes in Binaries and Galactic Nuclei*, Springer, 364.
- Hayashi, C., Narita, S., & Miyama, S.: 1982, *Prog. Theor. Phys.* **68(6)**, 1949.
- Li, Z-Y. & Shu, F. H.: 1996, *Astrophys. J.* **472**, 211.
- Lowe, S. A., Roberts, W. W., Yang, J., Bertin, G., & Lin, C. C.: 1994, *Astrophys. J.* **427**, 184.
- Lynden-Bell, D. & Pineault, S.: 1978a, *Mon. Not. R. Astron. Soc.* **185**, 679.
- Lynden-Bell, D. & Pineault, S.: 1978b, *Mon. Not. R. Astron. Soc.* **185**, 695.

- Mestel, L.: 1963, *Mon. Not. R. Astron. Soc.* **126**, 553.
- Penrose, R.: 1998, in *Black Holes and Relativistic Stars* (Chicago: University of Chicago Press), 103.
- Shu, F. H.: 1977, *Astrophys. J.* **214**, 488.
- Shu, F. H., Laughlin, G., Lizano, S., & Galli, D: 2000, *Astrophys. J.* **535**, 190.
- Tassoul, J.: 1978, *Theory of Rotating Stars*, (Princeton: Princeton University Press).
- Toomre, A.: 1977, *ARA&A* **15**, 437.
- Toomre, A.: 1982, *Astrophys. J.* **259**, 535.

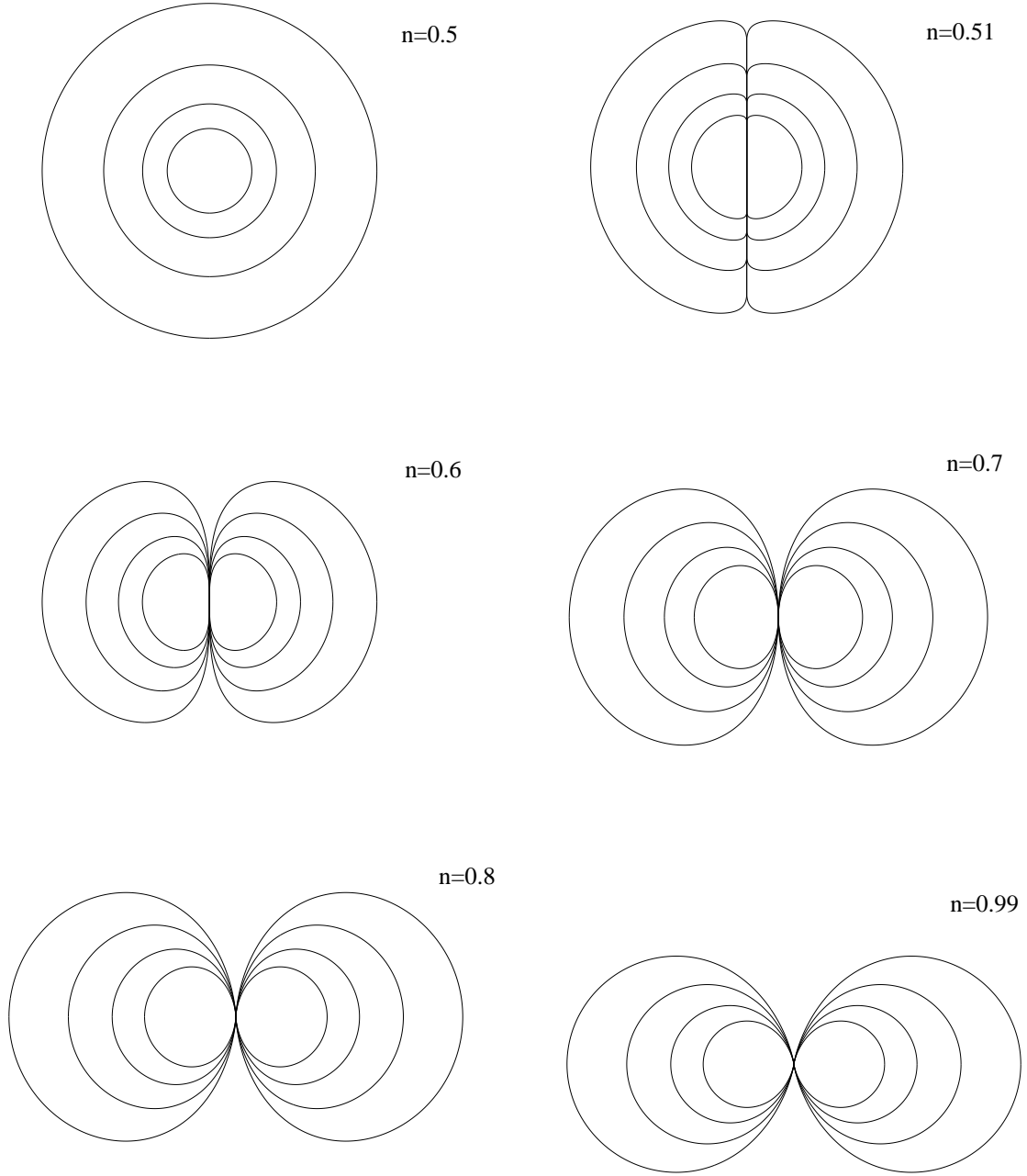


Fig. 1.— Meridional cross section of constant energy surfaces for  $\gamma = 1/3$ . The contours corresponds to 1, 2, 4, and 8 times some reference value. The allowed values of gravitational index range from  $n = 2\gamma/(1 + \gamma) = 0.5$  to  $n = 1$ .

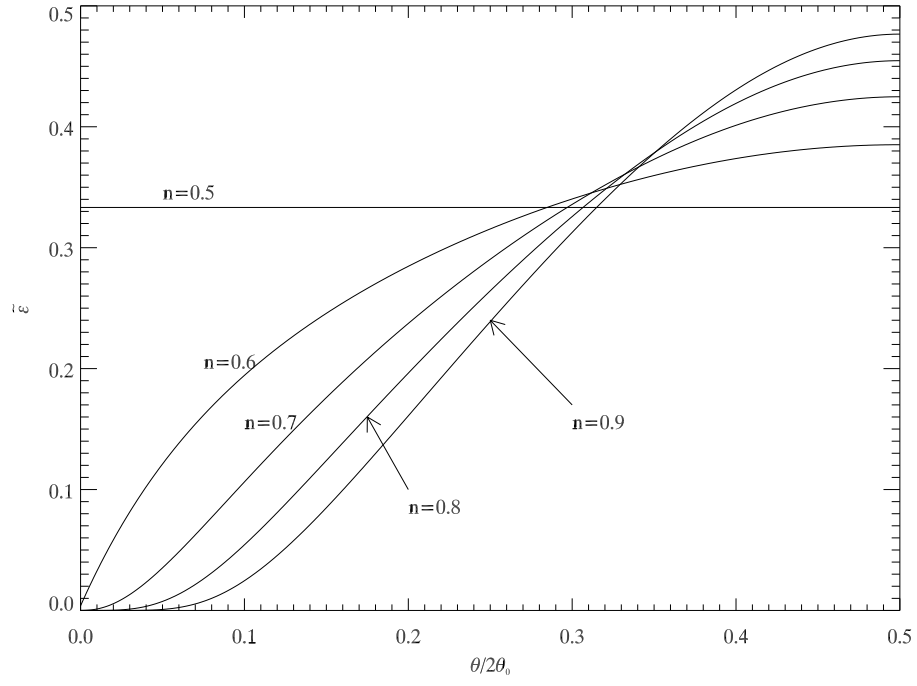


Fig. 2.— Rescaled energy density  $\hat{\epsilon}$  as a function of polar angle for  $\gamma = 1/3$ . The minimum gravitational index  $n = 0.5$  corresponds to a nonrotating sphere with constant  $\hat{\epsilon}$ . As  $n$  increases, energy is redistributed toward the midplane.

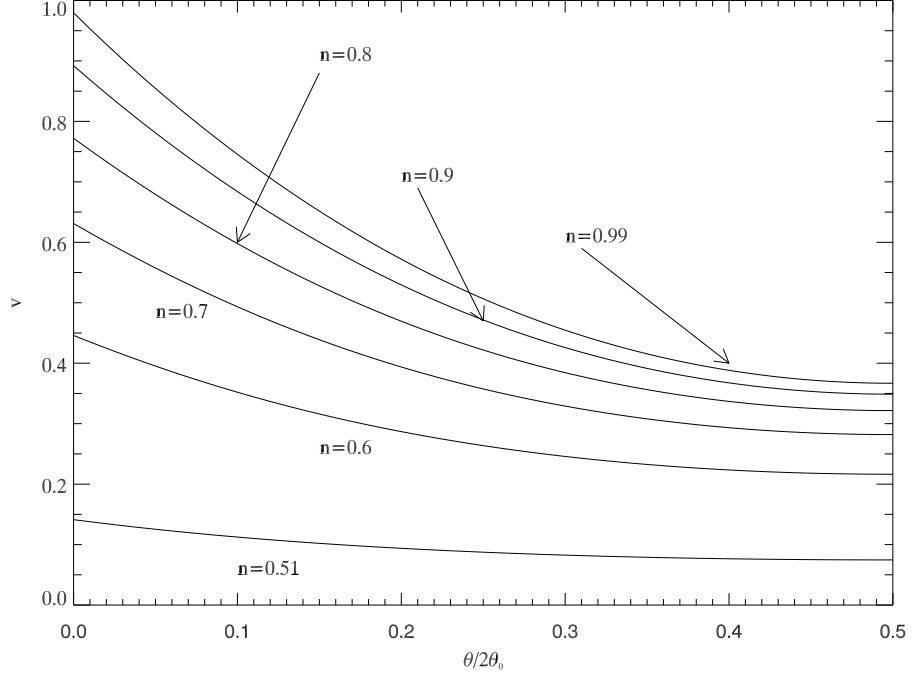


Fig. 3.— Linear rotational velocity as a function of polar angle for  $\gamma = 1/3$ .

Table 1. Critical Velocities for SID and SIT as a Function of Sound Speed Squared

$\gamma$	SID $v_c$	SIT $v_c$
0.0	0.438	0.439
0.1	0.415	0.414
0.2	0.398	0.395
0.3	0.381	0.375
0.4	0.366	0.347
0.5	0.351	0.313
0.6	0.339	0.276
0.7	0.327	0.235
0.8	0.316	0.190
0.9	0.306	0.132
1.0	0.298	0.050